



Swelling phenomena in anode wires aging under a high accumulated dose

T. Ferguson^a, G. Gavrilov^b, V. Gratchev^c, J.M. Dalin^d, A. Krivchitch^{b,*},
E. Kuznetsova^b, V. Lebedev^b, E. Lobachev^b, V. Polychronakos^c,
L. Schipunov^b and V. Tchernjatin^c

^a Carnegie Mellon University, Pittsburgh, PA 15213, USA

^b Petersburg Nuclear Physics Institute (PNPI), 188300 Gatchina, Russia

^c Brookhaven National Laboratory, Upton, NY 11973, USA

^d CERN, CH-1211 Geneva 23, Switzerland.

Elsevier use only: Received date here; revised date here; accepted date here

Abstract

We present results from an aging investigation of straw drift-tubes placed under sustained irradiation from a 2 Ci ⁹⁰Sr β -source. The aging phenomenon of gold-plated tungsten wires with diameters 25, 30 and 35 microns with accumulated charges up to 9 C/cm was studied thoroughly. Aging tests were carried out with different gas mixtures: 70%Xe+10%CO₂+20%CF₄, 60%Ar+30%CO₂+10%CF₄, 40%Ar+40%CO₂+20%C₂H₂F₄, and 60%Ar+30%CO₂+10%C₂H₂F₄. As a result of the aging process, the gold coating on the wires was damaged, and the wire diameter increased. For the first two gas mixtures, the wire swelling effect was concentrated only in the center of the irradiated zone. In comparison, the performance deterioration in the mixtures containing C₂H₂F₄ proved to be quite different. The gold coating on the wires was damaged, but outside of the irradiating area. Large deposits were found on the wire surface, both in the vicinity of the irradiated zone and downstream of the gas flow. All deposits contained tungsten and oxygen, resulting in the local increase of the wire diameter by 36% (from 30 to 41 μ m). Our data show that both aforementioned aging effects have a similar reason: the swelling of the wire material that creates forces within the anode wire and cracks the gold coating.

© 2001 Elsevier Science. All rights reserved

Keywords: aging; intensive irradiation; wire swelling; oxidation, tungsten.

^{*}) Corresponding author: A.Krivchitch, E-mail address kriv@rec03.pnpi.spb.ru Fax (007)-812-71-379-76; phone (007)-812-71-460-42.

1. Introduction

Aging effects usually result from surface degradation of the anode and cathode electrodes and occurs in the form of “deposits” [1]. The principal explanation for these mechanisms can be couched in terms of plasma chemistry. Different types of

phenomenon of a new aging mechanism and show that oxygen plays a very important role in the wire aging process under a high accumulated dose. Second, we propose that the tungsten oxidation process can explain anode wire swelling. Our discussion will be restricted to anode swelling as a phenomenon, which is intrinsically interesting and could be highly relevant for physicists investigating wire aging, both under experimental conditions and

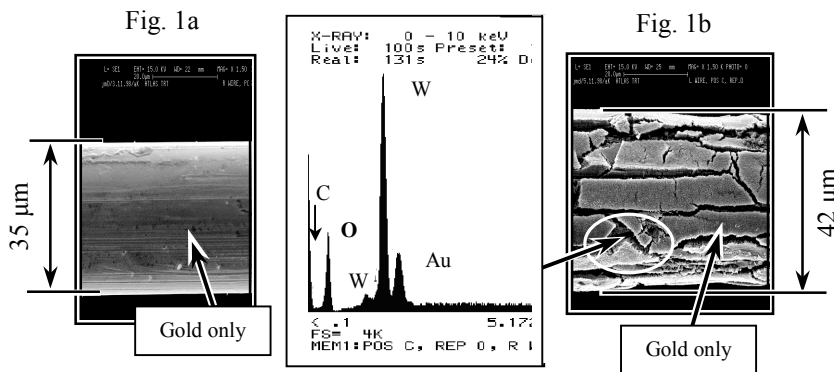


Fig. 1. Anode wire swelling effect. The scale ($20\ \mu\text{m}$ length) is indicated as a white line at the top of Figs. 1a and 1b. The arrow in the center plot indicates the location of possible carbon content. Results of SEM examination of the wire surface in the non-irradiated zone and in the center of irradiation are presented in Figs. 1a and 1b.

chemical radicals and ions produced in the gas avalanche near the anode wire cause the plasma reactions, leading to anode wire and cathode deposits. Some time ago, a new aging mechanism of the anode wire – the swelling of the wire under high-accumulated dose – was observed for the first time [2]. It was a new, unexpected process causing deterioration of gas detectors.

The principal difference between the anode wire-swelling phenomenon and the well-known polymerization mechanism of aging is that in the former, the forces are applied from within the wire, breaking the gold coating. As a result of this process, the wire diameter increases [2] (see Fig. 1). Also, an intense concentration of oxygen was observed on the open tungsten surface.

We surmise that the anode-swelling phenomenon is quite complicated and needs more investigation. For this reason, we are trying to describe just the general features of this process, which is not yet entirely understood. Our goal is to show the interconnection between the main causes of both the anode wire swelling and the development of aging.

This article has two main goals. The first is the presentation of experimental data, which confirm the

phenomenon of a new aging mechanism and show that oxygen plays a very important role in the wire aging process under a high accumulated dose. Second, we propose that the tungsten oxidation process can explain anode wire swelling. Our discussion will be restricted to anode swelling as a phenomenon, which is intrinsically interesting and could be highly relevant for physicists investigating wire aging, both under experimental conditions and

2. Test setup and data analysis

2.1. Test setup

The data were obtained during aging tests of straw-tubes [3] with different gas mixtures. The aging studies were performed at PNPI (St. Petersburg) using the Aging Test Station (ATS) [2]. The degradation test of the detector was carried out using a $2\ \text{Ci}\ ^{90}\text{Sr}$ β -source. The width of the β -source beam is about $\text{FWHM} = 1.8\ \text{cm}$. The straw-tubes used in our investigations had a diameter of $4\ \text{mm}$. The cathode consisted of a $50\ \mu\text{m}$ carbon-coated kapton film. The anode wires we have used were made of gold-coated tungsten with different diameters, delivered to us by our colleagues at BNL, DESY (wire made by California Wire, used in HERA-B Outer Tracker), and PNPI.

The gas flow in all the tests was $0.5 \text{ cm}^3/\text{min}$, or five straw volumes per hour. To avoid both air and water vapor penetration into the straws from the atmosphere, we placed the set of straws in a sealed box blown over by argon (see Fig. 2). Measurements of the straw-tube properties were made every few

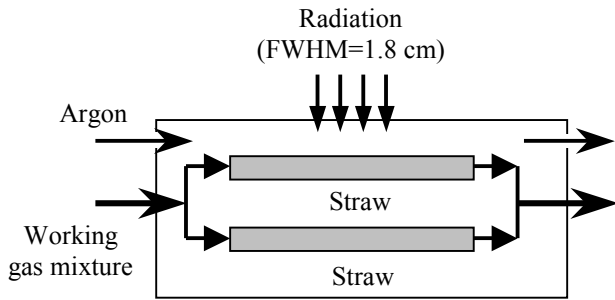


Fig. 2. Setup of straws for aging tests.

days during the exposure [2]. In order to monitor the gas gain, we scanned a collimated ^{55}Fe X-ray source along the straw length. The irradiated zone was especially scrupulously monitored; its length of 2.5 cm was scanned in 5 mm steps. The reference point was placed 4 cm away from the gas inlet edge of the straw-tube, which was located 14 cm from the center of the irradiated zone.

2.2. Choice of the working point

To illustrate how the high-voltage operating point was chosen, we have provided, in Fig.3, direct measurements of the current per wire for one of the gas mixtures used ($60\%\text{Ar}+30\%\text{CO}_2+10\%\text{CF}_4$). The current behavior was measured for two different rates, obtained at two different distances of source from the straw. The first source, which was at a 3-mm distance from the straw, was used during the real aging tests. The rate of the second source, which was placed 33 mm from the straw, should be so small that the expected space charge affecting the gas gain drop would be practically negligible. The gas gain values have been calculated for two current densities.

The effect of the space charge manifests itself as a difference between these two plots. This difference is due to the high intensity of irradiation. With the less intense irradiation, the nominal gas gain of 1×10^5 would be achieved at 1.65 kV. To approximate real experimental conditions as fully as possible, we chose the high voltage to compensate for the space charge effect, which decreases the gas gain under intense irradiation in the center of the irradiation area. This forced us to perform our aging tests at 1.74 kV, which put non-irradiated wires or parts of a wire at too high a voltage, or too high a gas gain. That resulted in nominal gas gain that was almost two

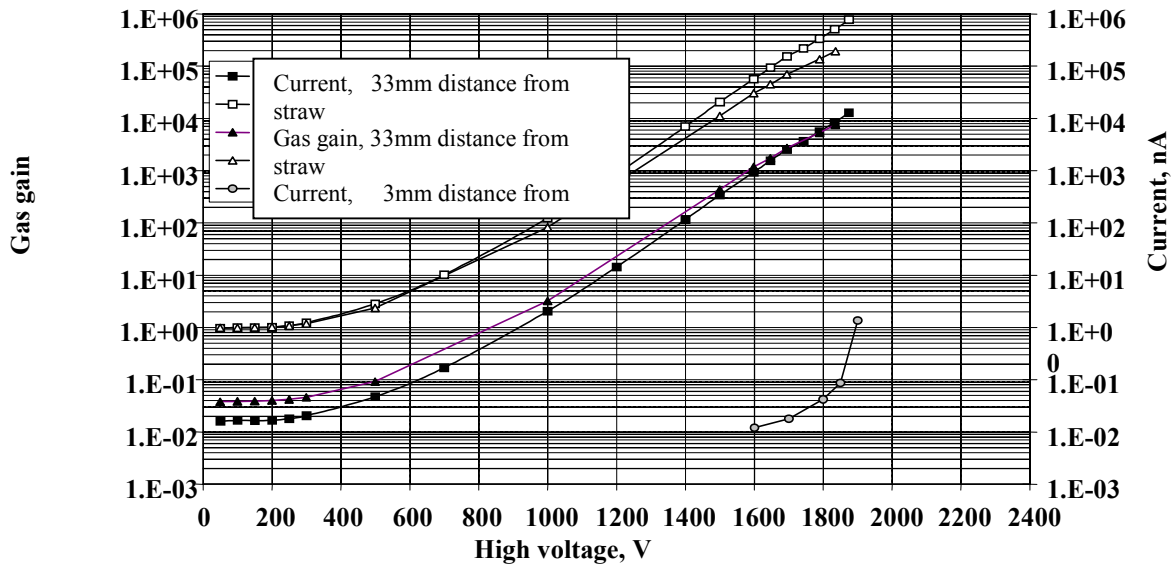


Fig.3. Gas gain dependence on the high voltage.

times higher at the non-irradiated section of the straw than at the irradiated section. This must be taken into account in the analysis of the data obtained.

2.3. Data analysis

The aging run conditions are presented in Table 1. Data for aging occurring only in the irradiated zone are shown with white background; data for aging occurring outside of the irradiated zone are shown with a gray background.

To analyze the anode surface after aging, we used a scanning electron microscope with X-ray emission (0-10 keV) spectroscopy (SEM/XEM). The SEM/XEM analysis yielded information on the morphology of the wire surface and the atomic composition of the surface layer.

accumulated oxygen reacts with the tungsten to cause the wire-swelling effect. However, note that the NRA and SEM/XEM methods successfully complement each other.

3. Aging test results

3.1. Aging properties of the straw drift-tubes after accumulation of 3.6 and 9 C/cm operated with a 70%Xe+10%CO₂+20%CF₄ gas mixture.

Aging studies of the straw-tubes using a 70%Xe+10%CO₂+20%CF₄ gas mixture have been performed [2]. Under a high-accumulated dose (about 9 C/cm) and a dose rate corresponding to 1.7 μA/cm, a new anode wire aging mechanism – the swelling of

Table 1

Gas mixture	Gas gain	Wire diameter [μm]	Rate [C/cm] per day	Total accumulated charge [C/cm]	Gas flow rate	
					Volume per hour	Linear velocity [cm/min]
70%Xe+10%CO ₂ +20%CF ₄	3×10 ⁴	35	0.15	9.0	5	4
70%Xe+10%CO ₂ +20%CF ₄	3×10 ⁴	35	0.16	3.6	5	4
60%Ar+30%CO ₂ +10%CF ₄	10×10 ⁴	30	0.17	1.5	5	4
60%Ar+30%CO ₂ +10%CF ₄	10×10 ⁴	25	0.17	1.5	5	4
60%Ar+30%CO ₂ +10%C ₂ H ₂ F ₄	10×10 ⁴	30	0.17	1.5	5	4
40%Ar+40%CO ₂ +20%C ₂ H ₂ F ₄	10×10 ⁴	35	0.17	1.5	5	4

In order to provide a quantitative evaluation of the distribution of light elements in the gold coating of the wires, we also conducted a nuclear reaction analysis (NRA) [4]. The NRA has a spatial resolution of about 4 mm, which is determined by the beam width. This means that the oxygen observed with the NRA reflects both the amount accumulated inside of the gold coating and the amount due to tungsten oxide in the cracks. The SEM/XEM analysis has a better spatial resolution (less than 1 μm) but can't provide a quantitative evaluation of the element content in the depth of the material. This is practically impossible because of the strong X-ray absorption by the wire material. Therefore, for the moment, we cannot estimate which part of the

the wire – was observed [2]. The results of a SEM/XEM examination of the wire surface have shown that in the center of the irradiated zone, the gold coating was broken, and the wire diameter increased by 20% from 35 μm to 42 μm.

The NRA evidently demonstrated both the key role of oxygen in the anode wire swelling mechanism and the kinetics of oxygen transportation into the depth of the gold coating. It has been shown that the average concentration of oxygen at the beginning of irradiation is about $1 \cdot 10^{21}$ at/cm³. The total amount of oxygen collected in the wire increased more than 20 times than that in one of the non-irradiated wires after an accumulation of 9 C/cm in the center of the irradiation zone. Moreover, the maximum value of

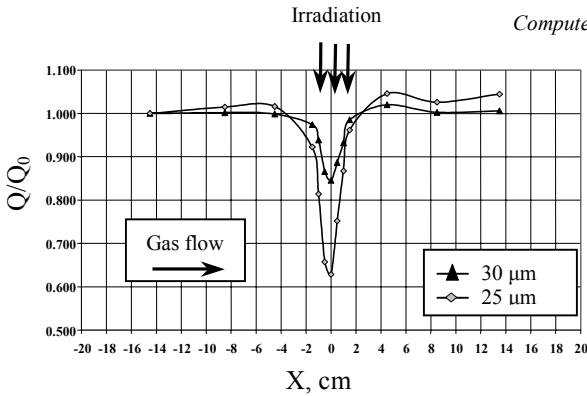


Fig. 4. Gas gain distribution along the straw for different wire diameters – 25 and 30 μm .

oxygen concentration in the gold coating increased by up to 10 times and achieved a very high value of $1 \cdot 10^{22}$ at/cm³.

Direct correlation between the anode wire diameter and the distribution of oxygen concentration along the wire has been demonstrated in [5]. Both their positions and shapes are strongly correlated and in good agreement with the beam position.

To study the early stage of the swelling, we stopped irradiation in the next test when the total accumulated charge was 3.6 C/cm. The results properly confirmed the correlation between the wire

Some deposits on the wire surface were observed, but only outside of the irradiated zone towards the gas outlet [2,5]. Tungsten and oxygen were detected in these deposits.

3.2. Influence of the wire diameters (25 and 30 μm) on the aging properties of straw drift-tubes operating with a gas mixture of 60%Ar+30%CO₂+10%CF₄.

Fig.4 shows the dependence of the gas gain ratio on the position along the wire for straws with anode wire diameters of 25 and 30 μm . As shown, we did not obtain any signs of aging from the inlet side of the straw. The gas gain dropped 2-3% on the outlet side of the straw-tube. In the center of the irradiation zone, evidence of significant aging degradation was found: the gas gain decreased about 37% and 18%, respectively, for the two wire diameters. The 25 μm diameter wire aged twice as rapidly as the 30 μm wire.

We also found a direct correlation between the anode wire diameters (Fig. 5) and the distribution of oxygen concentration along the wires (Fig. 6). In the center of the irradiated zone, the wire diameter increased by 4% (from 30 μm to 31.2 μm) after a

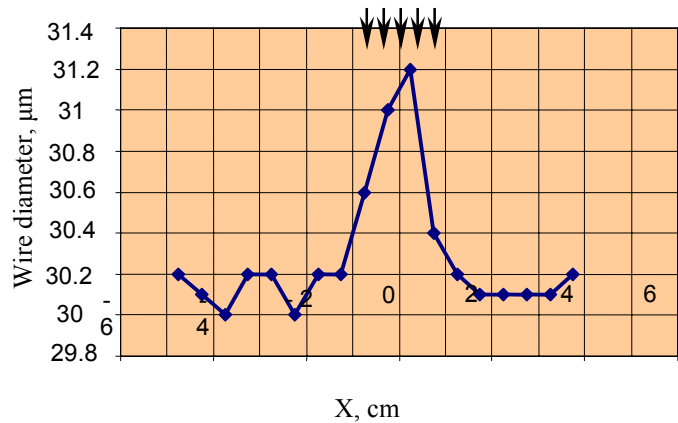
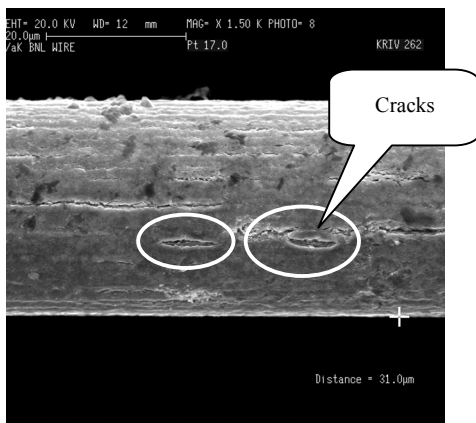


Fig. 5. (Left) Result of an SEM examination of the anode wire surface in the center of the irradiated zone. The scale (20 μm length) is indicated as a white line on the top part of figure. (Right) The anode wire diameter along the wire. The anode wire swelling effect is 1.2 μm for the 60%Ar+30%CO₂+10%CF₄ gas mixture. Wire diameter was 30 μm .

diameter and oxygen concentration. In the center of the irradiated zone, the wire diameter increased by 6% (from 35.3 μm to 37.3 μm).

charge accumulation of 1.6 C/cm. Thus, the wire-swelling effect is located only in the center of the irradiation zone.

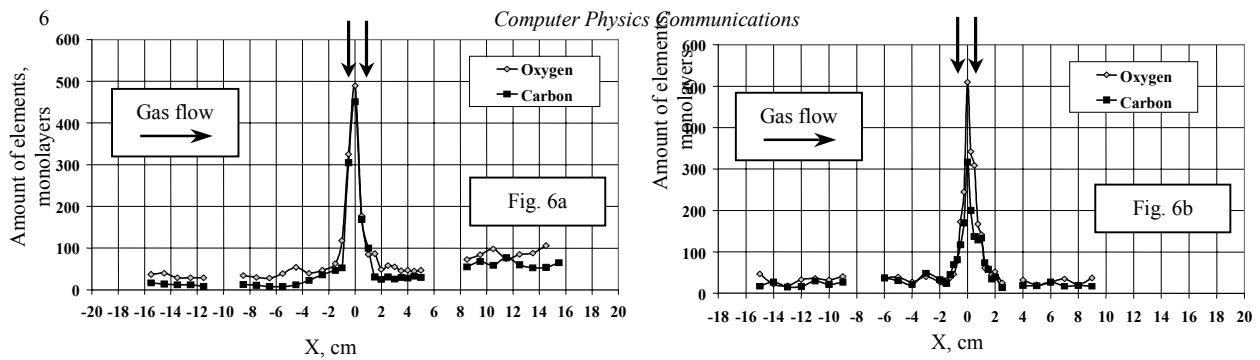


Fig. 6. The distribution of oxygen and carbon content along the wire with a diameter of 30 μm (Fig. 6a) and 25 μm (Fig. 6b). A 60%Ar+30%CO₂+10%CF₄ gas mixture was used.

The SEM/XEM analysis showed that the damaged tungsten surface contains a large amount of oxygen in the center of the irradiation zone. These data are a good match with the results presented in section 3.1 for the Xe/CO₂/CF₄ gas mixture.

The results obtained by NRA are presented in Fig. 6 for different points along the wire. After irradiation of the wires, the amount of oxygen and carbon is noticeably increased. We conclude that oxygen and carbon have penetrated the gold coating of the wire. In the center of the irradiation zone, the total amount of oxygen collected in the gold has increased more than 18 times in comparison to the non-irradiated wire. Moreover, the maximum value of the oxygen peak concentration increased up to 15 times, reaching a high value of $8 \cdot 10^{21}$ at/cm³ for the 30 μm wire (see Fig. 7a). For the 25 μm wire (Fig. 7b), this value did not exceed $6 \cdot 10^{21}$ at/cm³. As this discrepancy suggests, oxygen penetrated into the

may partially explain why the gas gain fell twice as fast in the 25 μm wire as in the 30 μm wire.

3.3. Aging of the straw drift-tubes with gas mixtures containing C₂H₂F₄.

It is important to note the high level of similarity between the results obtained for the two investigated gas mixtures containing C₂H₂F₄ (60%Ar+30%CO₂+10%C₂H₂F₄ and 40%Ar+40%CO₂+20%C₂H₂F₄). The main difference between them was the intensity of the wire aging, which was higher for the second gas mixture [6,7].

The aging processes developed mostly in two areas along the wire: in the center of the irradiation zone and downstream in the gas flow direction. In the center of the irradiation zone, the aging degradation was not so significant, and the decrease in gas gain did not exceed 2-3% (see Fig. 8). A larger gas gain

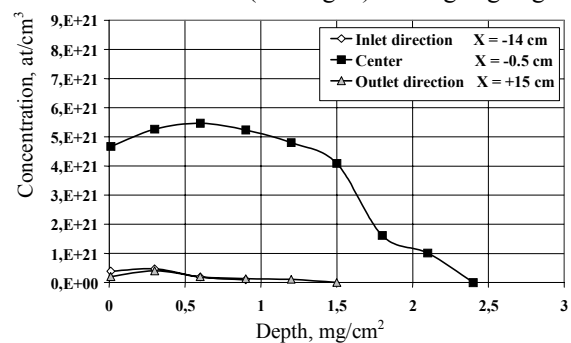
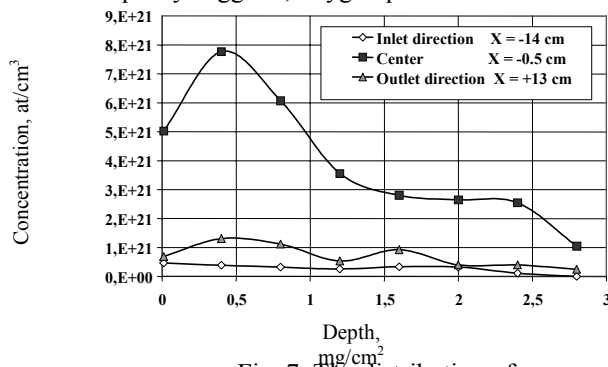


Fig. 7. The distribution of oxygen concentration as a function of depth into the wires with diameters 30 μm (Fig. 7a) and 25 μm (Fig. 7b).

25 μm wire more deeply than the 30 μm wire. This

reduction (7-8%) occurred outside of the irradiation zone.

In the center of the irradiated zone ($|X| \leq 1$ cm), the gold coating was unbroken, and the wire diameter did not increase (see Fig. 9). SEM/XEM analysis of the wire showed an absence of deposits on the surface. However, in the vicinity of the irradiated zone ($X = +1.25$ cm), a very thin layer of tungsten oxide was observed on the wire surface. Such deposits caused a small increase in the wire diameter in very small local areas (a few tenths of microns, see Fig. 9c), compatible with the gas gain drop of 2-3%.

localized decrease in gas gain (at least in a few instances) at these points on the wire. The appearance of such deposits makes the wire surface rougher rather than smoother; this explains the fast rise of dark current versus accumulated dose [6] and the gas gain drop of about 8% for $X \geq +1$ cm (Fig. 8).

Fig. 11 presents the results obtained by NRA at different points along the wire. After irradiation of the wire, the amount of oxygen and carbon had noticeably increased. Moreover, it was found that the

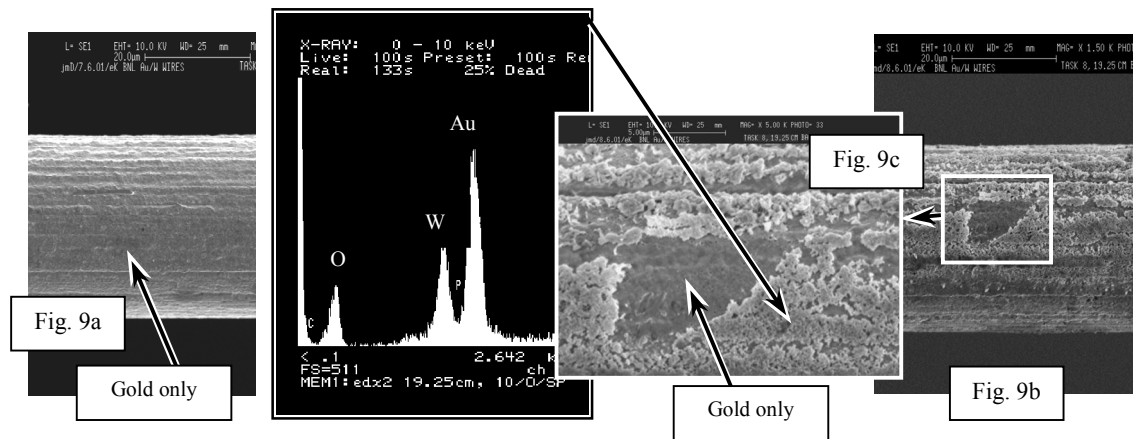


Fig.9. Results of SEM/XEM examination of the wire surface in the center of the irradiated zone. The distances between the center of the irradiated area and the gas outlets are $X = -0.5$ cm (Fig. 9a) and $X = +1.25$ cm (Fig. 9b). Fig. 9c shows the magnified fragment from the wire surface to emphasize the thin film of deposits containing tungsten and oxygen that covered the gold surface of the wire.

The scales (20 μm and 5 μm) are indicated by white line at the top of figures.

In this area, $X = [-1.5; +1.5]$ cm.

The spatial structure of the deposits, which were found on the wire surface outside of the irradiated zone towards the gas outlet, was quite different in comparison to those of the gas inlet section of the wire (Fig. 10). These deposits looked like both cracked thick films and blisters. Some of them looked like a volcano after eruption (Fig. 10a). The quantity of deposits was so large that they caused a local increase in the wire diameter from 30 μm up to a maximum of 41 μm (Fig. 10c). This resulted in a

distribution of oxygen concentration along the wire had a multi-peak structure. The first peak was at the center of the irradiation area, with the tail extending downstream along the gas flow direction a distance of $\Delta X = 10$ cm toward the gas outlet.

This means that active radicals created in the irradiated zone were not concentrated only inside this area. Instead, they spread outside this zone with the gas flow and reacted with the wire material, causing a strong contamination of wire sections near the gas outlet, far from the irradiated area.

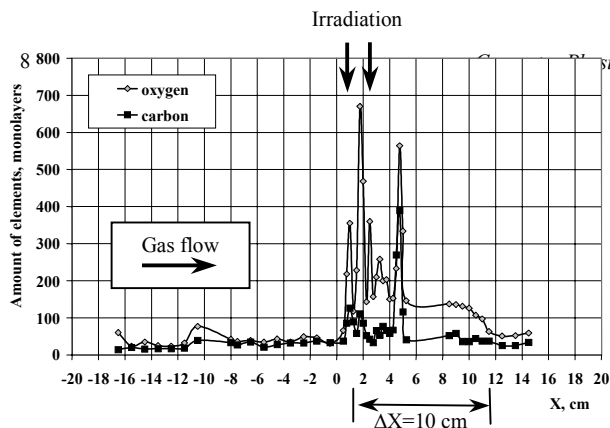


Fig.11. The distribution of oxygen and carbon content along the wire.

We determined that the total amount of oxygen collected in the gold increased by more than 15 times in the center of the irradiation zone and about 3-4 times outside of it ($+1 \leq X \leq +10$ cm). Moreover, the peak oxygen concentrations achieved very high values of $1 \cdot 10^{22}$ at/cm³ and $6 \cdot 10^{21}$ at/cm³, respectively. The maximum peak concentration of carbon before irradiation was about $2 \cdot 10^{20}$ at/cm³ and did not exceed $1.2 \cdot 10^{21}$ at/cm³ after. Thus, the concentration of oxygen in the wire was about 10 times higher than that of carbon.

4. Discussion of results

4.1. Comparison of data.

The experimental data presented in sections 3.1 and 3.2 are quite different from the results presented in section 3.3. In the first experiments, we observed wire swelling in the center of the irradiated zone and some amount of tungsten-oxygen containing compounds, distributed along the wire asymmetrically with respect to the gas flow direction. The wire swelling caused a gas gain decrease in the center of the irradiated zone.

In the experiments with gas mixtures containing C₂H₂F₄, we did not observe the anode wire swelling effect directly. Moreover, the wire diameter remained practically constant in the center of the irradiated zone. However, as a result of the aging process, the gold coating on the wires was damaged, and a large quantity of deposits were observed on the wire surface. All deposits contained tungsten and oxygen and were distributed mainly outside of the center of the irradiation area along the wire in the gas flow

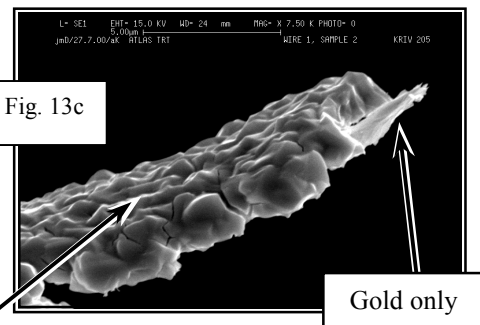
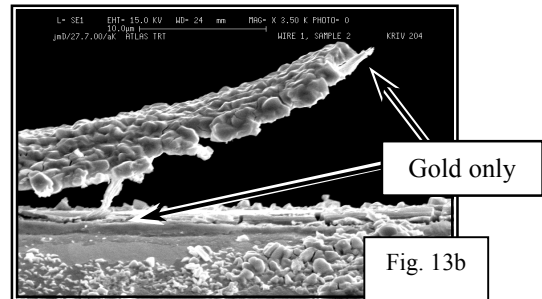
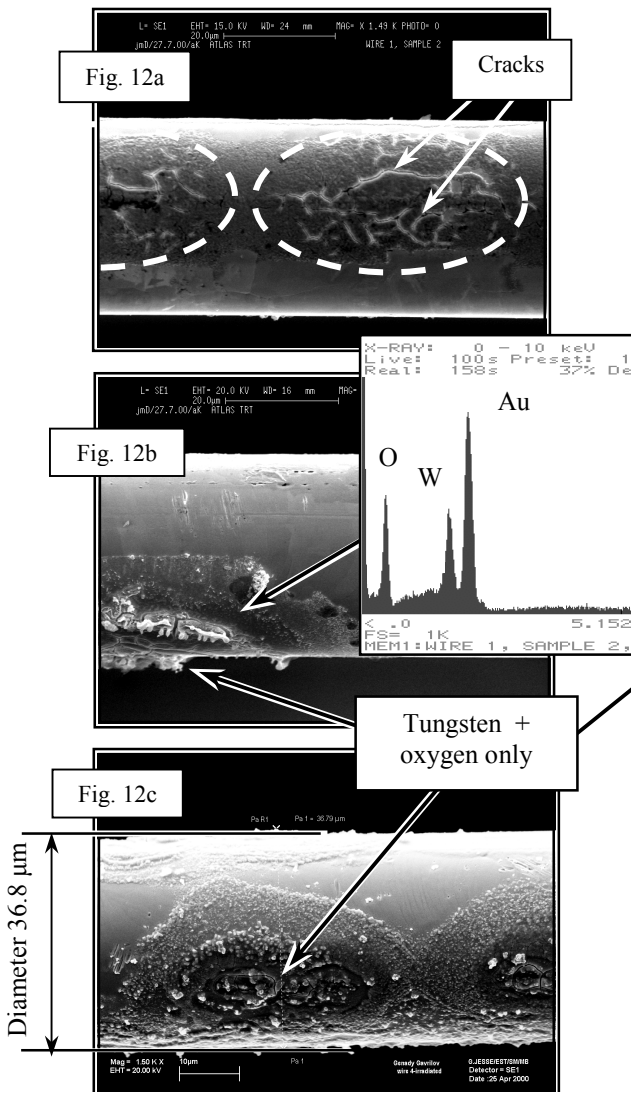


Fig.12. Results of a SEM/XEM examination of the anode wire surface in a few neighboring points which are in area $X = - [1.75 - 1.12]$ cm towards the gas inlet direction.

Fig.13. The results of a SEM/XEM examination of the wire surface in the center of the irradiated zone $X = - 0.25$ cm. A thick film of deposit containing tungsten and oxygen can be seen on the wire surface.

The scales (20 μm, 10 μm and 5 μm) are indicated by a white line on the top of figures 13a, 13b and 13c correspondingly.

direction. These deposits caused a local increase of the wire diameter from 35 μm up to 40.2 μm (for the gas mixture with 20% $\text{C}_2\text{H}_2\text{F}_4$), which directly explains the decrease in gas gain outside of the irradiated zone.

Practically all deposits observed in the experiments contained tungsten and oxygen. Since the only source of tungsten in the straw-tube is the wire material, we assume the following three-stage mechanism of wire deterioration (see Figs. 12-14). This mechanism has already been discussed in more detail for the 70%Xe+10%CO₂+20%CF₄ gas mixture in [2]. We will illustrate our discussion using the data obtained with the gas mixture containing 20% $\text{C}_2\text{H}_2\text{F}_4$.

4.2. Schematic mechanism of aging development.

At the beginning of the process, the pores in the gold crystallite structure of the wire coating can grow and develop under the influence of sustained irradiation and due to gold etching. This provides locally favorable conditions for active oxygen with broken bonds, and for more complicated chemical radicals, to penetrate through the gold to the tungsten. As a result, the gold layer becomes more porous and covered with cracks, as shown in Fig. 12a, where a SEM micrograph of the irradiated anode wire surface is shown.

Second, oxygen penetrates through the pores and cracks underneath the gold layer and, we assume, oxidizes the tungsten. Other compounds are also created there. This causes a swelling of the tungsten in the wire and, as a consequence, the forces produced within the wire break the gold coating. Then aggressive radicals, including active oxygen, penetrate through the already opened cracks in the gold layer and react directly with the tungsten. As a result, swelling of the tungsten develops in a domino effect, and the tungsten oxide emerges on the wire surface (Fig. 12b).

In the third stage, the locally damaged areas swell and join together, covering the wire surface with tungsten-oxygen compounds. As a consequence, the gold surface is damaged and covered with cracks (Fig. 12c). The circular geometry of the damaged area demonstrates the point-like character of the initial swelling. This leads us to conclude that the

tungsten oxidation starts at weaker points in the gold coating after these are damaged by the active plasma species. This causes the swelling of the wire material and a resulting spread of the tungsten oxide over the wire surface. As shown in Fig. 12c, the deposits cause a local increase of the wire diameter from 35 to 36.8 μm .

The following processes occur after an intensive creation of tungsten-oxygen compounds on the wire surface, as illustrated in Fig. 13. One can see that the forces created by these deposits are strong enough to rip a long piece of gold coating away from the wire surface. Of course, such wire surface damage stimulates micro-discharges and produces a strong rise in dark current. This scenario fits well with the results presented in [6].

The main difference between the experiments with CF₄ and $\text{C}_2\text{H}_2\text{F}_4$ gas mixtures is the very high yield of deposits per specific accumulated charge for gas mixtures containing $\text{C}_2\text{H}_2\text{F}_4$. We believe that for these gas mixtures (10% and 20% of $\text{C}_2\text{H}_2\text{F}_4$), the etching processes in the gold coating [2] and the deposit creation are more intense than for the other gas mixtures that displayed the wire-swelling effect. In this case, the tungsten-oxygen compounds travel to the wire surface so fast that the wire doesn't have enough time to swell.

4.3. Pathways for oxygen transportation through the gold layer.

It is possible to postulate the following possible pathways of oxygen (or other radicals) through the gold layer into the tungsten (see Fig. 14):

1. Diffusion into the layer of gold coating through the crystal lattice internodes, followed by oxidation of the tungsten.
2. The movement of oxygen through imperfections in the gold coating caused by the wire manufacturing, followed by oxidation of the tungsten.
3. These imperfections can increase and develop under the influence of the gold etching, which strongly attacks defects in the gold coating and results in its extension. This increases the transparency of the gold coating and opens a direct path for the oxygen or other chemical radicals to

reach the tungsten. In other words, etching may speed up the wire aging.

At present, we cannot convincingly say which of the above-mentioned pathways applies for our working conditions. We believe that the probability of oxygen transportation for each of the mentioned pathways strongly depends on many different factors, such as the wire-manufacturing technology, the

define specifications for the quality of wires, which are intended for use at high-irradiation conditions.

In spite of this, we have already obtained results that can help us reach important conclusions. Our data allow us to definitely state that manufacturing defects (imperfections) play a very important role in the development of damage to the gold wire coating. Experimental data presented in [2] demonstrate that

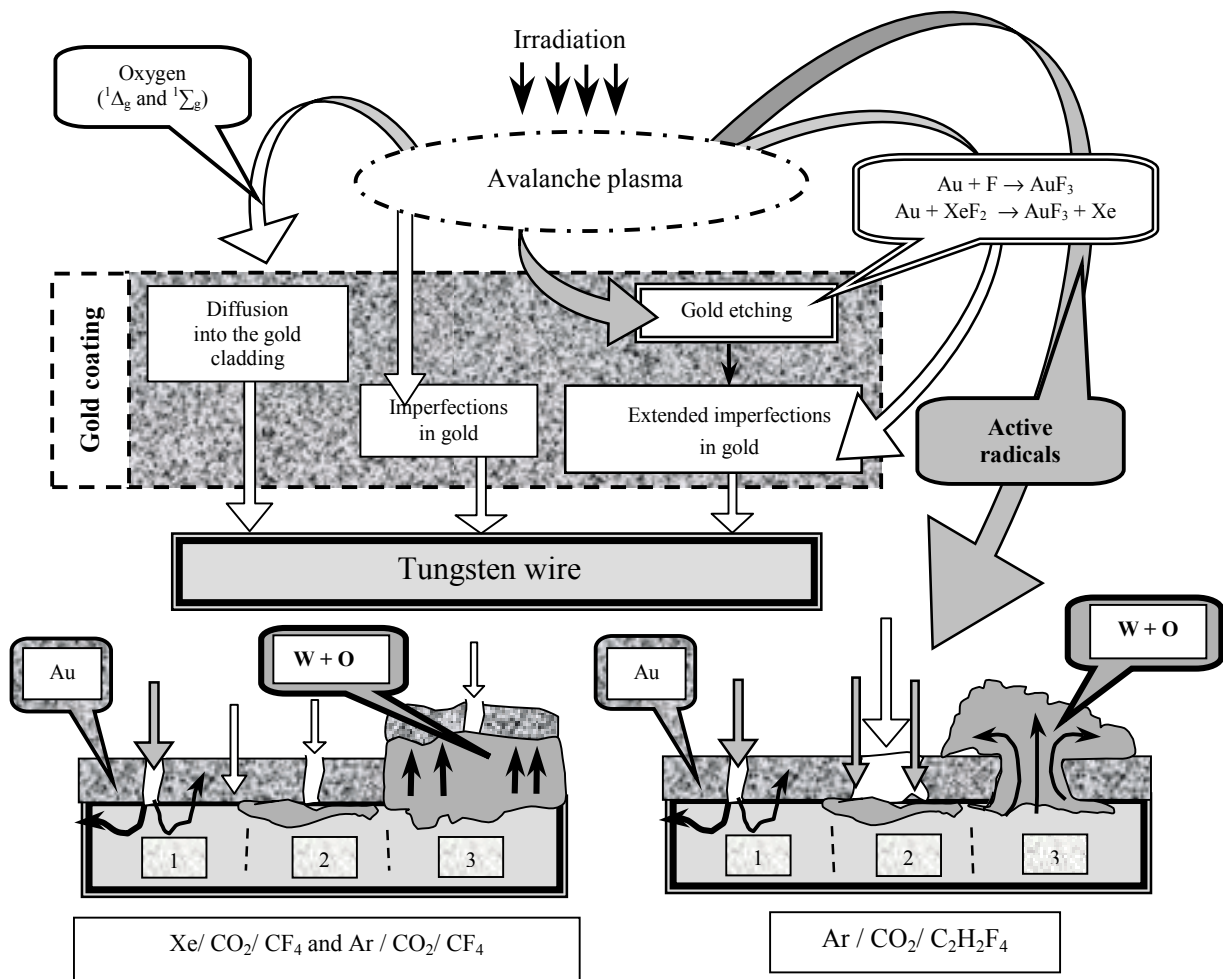


Fig. 14. Two different aspects of the wire swelling effect.

thickness of the gold layer, the gas mixture, the ionization dose, etc. Moreover, the primary cause of the cracks is open to interpretation because adequate evidence is not yet available. In other words, more study of the wire swelling effect is needed in order to

the gold layer is broken at particular points on the wire surface. The damage develops both at the point defects (pitting corrosions) and along the grooves caused by the drawing die during the wire manufacturing. This leads us to conclude that the oxygen penetrates the gold coating mainly at its

defect points, and, consequently, the tungsten oxide grows at these points first, exerting sufficient force there to breach the gold.

5. Conclusions

1. The wire-swelling effect was observed for two different gas mixtures: 70%Xe+10%CO₂+20%CF₄ and 60%Ar+30%CO₂+10%CF₄. Three different diameters of anode wire were used in these tests: 25, 30 and 35 μm. A direct correlation between the anode wire diameter and the distribution of oxygen concentration along the wire was demonstrated. In the center of the irradiated zone, the wire diameter increased by a few microns. Therefore, the wire-swelling effect is located at the center of the irradiated zone only.

2. A strikingly different wire-swelling effect was discovered for two other gas mixtures containing C₂H₂F₄ – namely, 60%Ar+30%CO₂+10%C₂H₂F₄ and 40%Ar+40%CO₂+20%C₂H₂F₄. Two diameters of anode wires were used in these tests: 30 and 35 μm. It was shown that the wire diameter remained practically constant in the center of the irradiated zone. As a result of the aging process, the gold coating on the wires was damaged, and a large number of deposits appeared on the wire surface. All deposits contained tungsten and oxygen and were distributed mainly outside of the center of the irradiated zone and along the wire toward the gas outlet. These deposits caused a local increase in the wire diameter by 36% (from 30 μm up to 41 μm) for the gas mixture with 10% C₂H₂F₄.

3. The gas mixtures containing C₂H₂F₄ components demonstrated asymmetrical behavior with respect to gas-gain degradation, deposit distribution, and oxygen concentration along the wire after irradiation. This led us to conclude that the gas avalanche creates different types of radicals than in the CF₄ mixtures. The chemical activity of some of them is so high that they easily penetrate the gold coating and react with the tungsten, finally causing a large amount of tungsten-oxygen compounds to form along the wire surface.

4. The XEM analysis of the wire surface did not show any visible traces of fluorine but only some traces of carbon. The NRA analysis showed some

amount of carbon inside of the wire coating. These are the reasons for our conclusion that the anode swelling effect can be explained mainly by tungsten oxidation in the wire.

5. The wire-swelling effect has two different facets, which were observed for gas mixtures containing CF₄ and C₂H₂F₄. Comparison of the wire-swelling data and the deposits distributed along the wire leads us to conclude that, in spite of the large differences between the conditions and results of the experiments, the cause of wire aging is the same – the swelling of the anode wire material.

Acknowledgements

We are very grateful to Prof. A. Vorobyov (PNPI) for his strong support of this work and his fruitful discussions of the results. We express thanks to V. Maleev (PNPI) and E. Ivanov (PNPI) for many productive discussions and help. We are very grateful to Jean-Michel Dalin (CERN) for his very friendly help in the SEM/XEM data analysis. We are very thankful to Yu. Lukjanov and V. Smolin for their kind help in the NRA of the data.

References

- [1] J.A. Kadyk, Nucl. Inst. and Meth. A 300 (1991) 436.
- [2] T. Ferguson, G. Gavrilo, A. Egorov, A. Krivchitch, E. Kuznetsova, V. Lebedev, L. Shipunov, Anode wire swelling - a possible phenomenon in anode wire aging under high-accumulated dose, accepted for publication in Nucl. Instr. and Meth. A, reference number 41300.
- [3] T. Akesson, et al., Electron identification with a prototype of the Transition Radiation Tracker for ATLAS experiment, Nucl. Inst. and Meth. A 367 (1995) 143.
- [4] G. Gavrilo, A. Krivchitch and V. Lebedev, Application of Nuclear Reaction Analysis for aging investigations of detectors, these proceedings.
- [5] T. Ferguson, G. Gavrilo, A. Krivchitch, E. Kuznetsova, V. Lebedev, L. Schipunov, The effect of oxygen on anode wire swelling under high-accumulated dose, Vienna Conference on Instrumentation 2001, Nucl. Instr. and Meth. A 478 (2002) 254.
- [6] G. Gavrilo, A. Krivchitch, E. Kuznetsova, V. Lebedev, L. Schipunov, E. Lobachev, Aging properties of the straw drift-tubes operating with gas mixture containing C₂H₂F₄, Preprint PNPI, No.2407 (2001).

- [7] G. Gavrilov, A. Krivchitch, E. Kuznetsova, V. Lebedev, L. Schipunov, E. Lobachev, Aging investigation of the straw drift-tubes using Nuclear Reaction Analysis, Vienna Conference on Instrumentation 2001, Nucl. Instr. and Meth. A 478 (2002) 259.

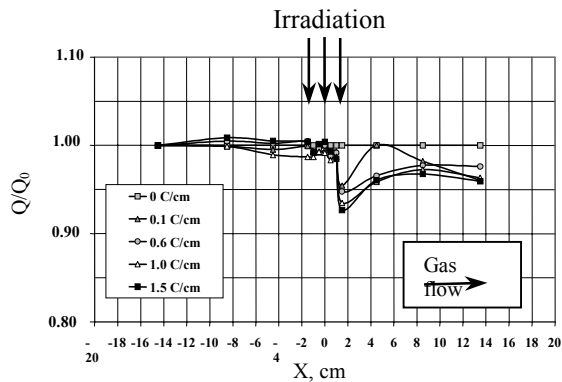


Fig.8. Gas gain distribution along the straw for different accumulated dose.

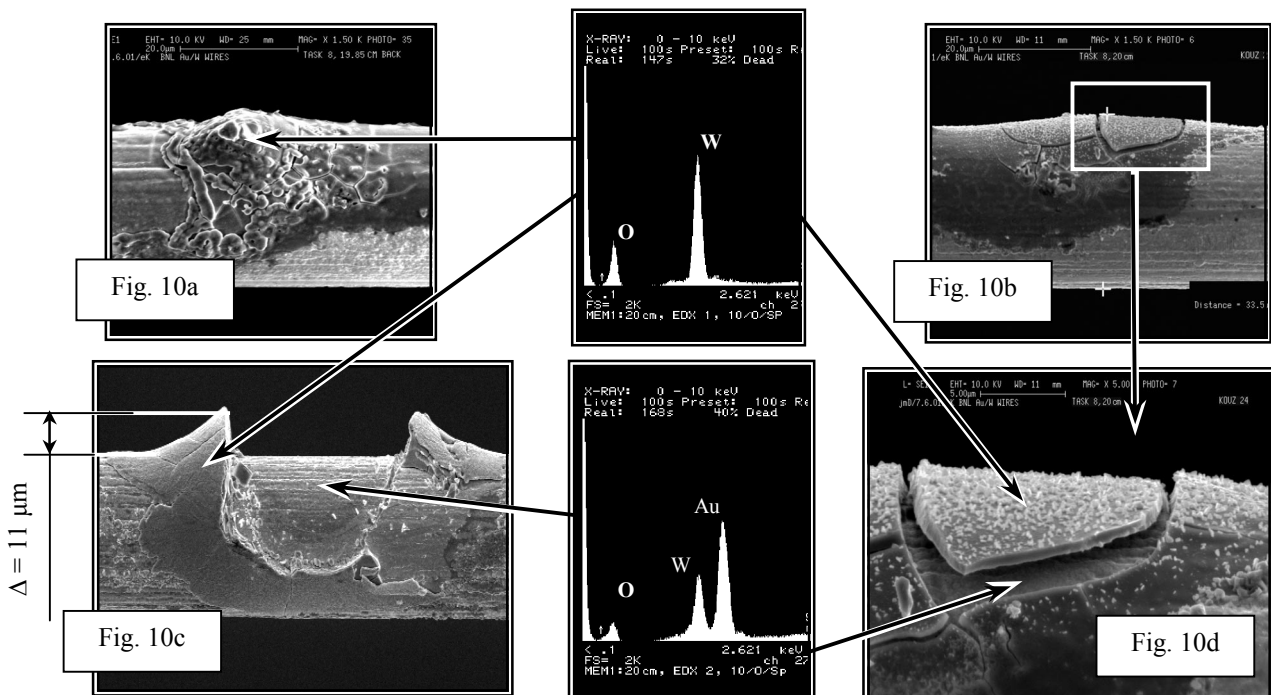


Fig. 10. Typical results of SEM/XEM examinations of an anode wire in a few neighboring points, which are in the vicinity of the irradiation zone downstream of the gas flow direction. The distances between the center of the irradiated area towards gas outlet are $X = +1.85$ cm (Fig. 10a), $X = +2.0$ cm (Fig. 10b), and $X = +2.4$ cm (Fig. 10c).

A fragment of the wire, which is indicated by the white box in Fig. 10b, is presented in Fig. 10d with larger magnification. The scale ($5 \mu\text{m}$) is indicated by a white line on the top part of Fig. 10d. A thick film of tungsten oxide is clearly observed above the gold coating of the wire.